

 Open access • Journal Article • DOI:10.1109/T-ED.1984.21511

A sensitivity analysis of SPICE parameters using an eleven-stage ring oscillator

— [Source link](#) 

J.M. Cassard

Institutions: National Institute of Standards and Technology

Published on: 01 Feb 1984 - IEEE Transactions on Electron Devices (IEEE)

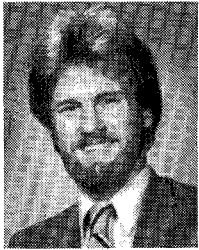
Topics: Ring oscillator, Electronic circuit simulation, Spice, Node (circuits) and Electronic circuit

Related papers:

- [A sensitivity analysis of SPICE parameters using an eleven-stage ring oscillator](#)
- [A Unified Statistical Model for Inter-Die and Intra-Die Process Variation](#)
- [Hypersensitive parameter-identifying ring oscillators for lithography process monitoring](#)
- [Ring oscillator with calibration circuit for accurate on-chip IR-drop measurement](#)
- [Variation-Sensitive Monitor Circuits for Estimation of Global Process Parameter Variation](#)

Share this paper:    

View more about this paper here: <https://typeset.io/papers/a-sensitivity-analysis-of-spice-parameters-using-an-eleven-54wzfgekji>



John S. Suehle (S'81-M'82) received the B.S. and M.S. degrees in electrical engineering from the University of Maryland, College Park, in 1980 and 1982, respectively. In 1981 he received a Graduate Research Fellowship with the National Bureau of Standards, Washington, DC. Since 1982 he has been working in the Semiconductor Devices and Circuits Division, National Bureau of Standards.

His research activities include developing analysis methods for microelectronic test chip data and characterizing semiconductor devices and fabrication processes through test structure measurements.

Mr. Suehle is a member of Eta Kappa Nu.



Loren W. Linholm (S'67-M'68) received the B.S. degree in electrical engineering from the University of California, Berkeley, in 1968, and the M.S. degree in electrical engineering from the University of Maryland, College Park, in 1973.

From 1963 to 1968 he was employed by the Naval Missile Center, Point Mugu, CA, in an engineering training program. In 1968 he began work for the Department of Defense, Ft. Meade, MD. His responsibilities included designing input protection devices for integrated circuits and

fabricating MOS prototype circuits. He was later responsible for establishing and operating an integrated circuit fabrication facility. Since 1978, he has been employed by the Semiconductor Devices and Circuits Division, National Bureau of Standards, Washington, DC, and currently heads the Integrated Circuit Test Structures Group. He is responsible for developing microelectronic test structures and analysis methods for characterizing integrated circuit fabrication processes.

Mr. Linholm is a member of Tau Beta Pi, Eta Kappa Nu, and the Electrochemical Society.



Karen Kafadar received the B.S. degree in mathematics, the M.S. degree in statistics from Stanford University, and the Ph.D. degree in statistics from Princeton University in 1979.

She was an Assistant Professor in the Statistics Department at Oregon State University and then joined the Statistical Engineering Division at the National Bureau of Standards in July 1980. She has published articles on statistical applications using robust methods and has a continuing interest in data analysis and graphical techniques.

Since May 1983, she has been with the Product Assurance Department at Hewlett-Packard Company in Palo Alto, CA.

A Sensitivity Analysis of SPICE Parameters Using an Eleven-Stage Ring Oscillator

JANET M. CASSARD

Abstract—SPICE is a circuit simulator which predicts node voltages and currents as a function of time from device model parameters. Model parameters are determined by the manufacturing process. Process-induced variations in these parameters occur within a chip or from chip to chip and cause corresponding variations in circuit performance. Values for the model parameters used in simulators are usually obtained from measurements on test structures which are found along the periphery of the circuit or in test chips located at several sites on the product wafer. Because of the spatial separation between test structures and the circuits of interest, differences between measured and simulated performance can occur. This paper presents examples of how well model parameters extracted from a test chip can predict the ac response of a dynamic circuit element (ring

oscillator) on the same wafer. Simulation results show which model parameters are critical to performance. A comparison between measurement and simulation results is given and the importance of intra-chip and intra-wafer parameter variations is discussed. For the samples tested, the polysilicon gate linewidth variation was determined to be the primary cause of the ring oscillator frequency variation.

NOMENCLATURE

Symbol	Units	Identification
$CGD0$	F/m	Gate-to-drain overlap capacitance per meter of channel length.
KP_n	A/V^2	$\left(\frac{\text{n-channel transconductance}}{V_D} \right) \left(\frac{L_n}{W_n} \right)$.
KP_p	A/V^2	$\left(\frac{\text{p-channel transconductance}}{V_D} \right) \left(\frac{L_p}{W_p} \right)$.

Manuscript received May 26, 1983. This work was supported in part by the Defense Advanced Research Projects Agency under Order 3882.

The author is with the Semiconductor Devices and Circuits Division, National Bureau of Standards, Washington, DC 20234.

L_n	μm	Channel length for n-channel devices.
L_p	μm	Channel length for p-channel devices.
LD	μm	Lateral diffusion.
t_{ox}	nm	Oxide thickness.
V_D	V	Drain voltage.
V_{DD}	V	Power supply voltage.
V_{SS}	V	Ground voltage.
$VT0_n$	V	Threshold voltage for n-channel devices.
$VT0_p$	V	Threshold voltage for p-channel devices.
W_n	μm	Channel width for n-channel devices.
W_p	μm	Channel width for p-channel devices.

I. INTRODUCTION

BEFORE fabricating complex VLSI circuits it is important to identify errors in the circuit design. The effectiveness of SPICE in simulating actual circuit performance from a set of device model parameters is influenced by process-induced variations that affect these input parameters. In this paper, the critical input parameters are identified, and the effect of their variation on the simulation is estimated. A test chip containing ring oscillators and test structures for extracting the model parameters for SPICE was designed and fabricated in a p-well CMOS bulk local oxide-isolated process at two silicon foundries using 5- μm design rules [1]. An automated parametric test system was used to measure the electrical model input parameters, and the nonelectrical parameters were determined from physical measurements. The mean and standard deviation of each parameter was determined. A manual test system was used to measure the frequency of an eleven-stage ring oscillator.

The ring oscillator was simulated, using SPICE 2G.4, to determine the sensitivity of the ac oscillation frequency to fixed model-parameter variations. The model parameters critical to the frequency of oscillation were identified, and measured variations in these critical model parameters were used to examine the variations in simulated frequency.

This paper compares the measured ring oscillator performance to the simulated performance. Differences between the measured and simulated oscillation frequency means are due to the inaccuracy of the SPICE model (e.g., in scaling), deficiencies in the design of the test structures used for extracting the SPICE parameters, and deficiencies in measurement methods. Differences between the measured and simulated ranges are due to intrachip and intra-wafer parameter variations. The results of this study show that measured variations in approximately one-fourth of the SPICE model parameters, those critical to ac response, provide an adequate model for the measured ring oscillator frequency range.

II. EXPERIMENTAL PROCEDURE AND RESULTS

The wafers studied contain 32 or 21 test chips for foundries *A* or *B*, respectively. Each chip includes identical MOSFET's systematically placed across the test chip,

TABLE I
A COMPARISON OF CRITICAL INPUT PARAMETER VALUES FOR
SAMPLES FROM TWO SILICON FOUNDRIES

Parameter	Value for sample Foundry	for A	Value for sample Foundry	for B
V_{DD}	5.00	V	5.00	V
L_p	5.00 \pm .19	μm	5.00 \pm .15	μm
L_n	5.00 \pm .27	μm	5.00 \pm .25	μm
t_{ox}	75.0 \pm 5.0	nm	87.5 \pm 2.5	nm
KP_n	33.9 \pm 0.5	$\mu\text{A}/\text{V}^2$	33.5 \pm 0.7	$\mu\text{A}/\text{V}^2$
LD	0.58 \pm 0.06	μm	0.90 \pm .09	μm
KP_p	14.0 \pm 0.3	$\mu\text{A}/\text{V}^2$	11.3 \pm 0.5	$\mu\text{A}/\text{V}^2$
W_n	78.2 \pm 0.3	μm	78.2 \pm 0.3	μm
$VT0_n$	0.96 \pm 0.02	V	0.82 \pm 0.06	V
$CGD0$	287 \pm 45	pF/m	355 \pm 46	pF/m
$VT0_p$	-0.88 \pm .01	V	-0.66 \pm .09	V

cross-bridge resistors [2], [3], capacitors, and ring oscillators. The chip was designed in a 2 by N probe pad configuration [4], [5] to maximize testing efficiency. The wafers were measured with an automated parametric test system, and test results were analyzed using statistical evaluation techniques [6]. The test methods for obtaining the model parameters for SPICE can be found elsewhere [7]–[9]. The test results for selected parameters are shown in Table I. A manual station was used to measure the ring oscillator frequency. A low-capacitance probe (0.1 pF) was used to probe the output in order to minimize the capacitive loading.

A ring oscillator was chosen for this analysis because it is a simple circuit, it is used widely on test chips for monitoring process variations, and its oscillation frequency is sensitive to SPICE model parameters. An eleven-stage ring oscillator was designed since initial simulations, for the process and design employed, indicated that the output waveform would achieve maximum oscillation amplitude for that odd number of stages. Also, a prime number of stages was chosen to help suppress the occurrence of harmonics that might otherwise occur for the relatively small number of stages employed [10].

The ring oscillator consists of three basic elements: an inverter, a NAND gate, and an output buffer. Ten inverters and one NAND gate are tied together forming the circuit. The NAND gate is used in place of one inverter to prevent multiple oscillations in the ring [10]. The six-stage output buffer is tied to one node of this ring. In each successive stage of the output buffer, the channel widths are twice as large as the previous stage to minimize the capacitive loading introduced by the measurement probe [11] and to make efficient use of silicon area. A block diagram of the ring oscillator is shown in Fig. 1 along with the circuit diagram of one inverter.

III. SIMULATIONS

To determine the sensitivity of SPICE simulations to device model parameter variations, two groups of simulations were performed. The first simulations determined the sensitivity of the frequency of the ring oscillator to a fixed variation in each model parameter. From this, a set of

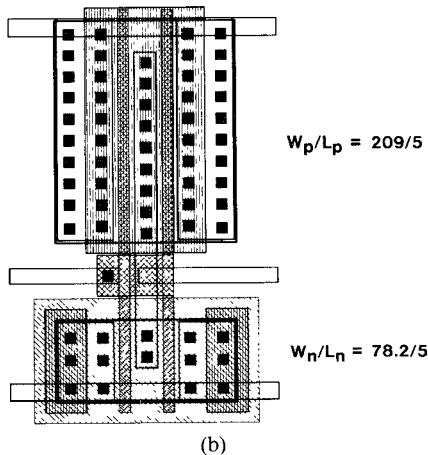
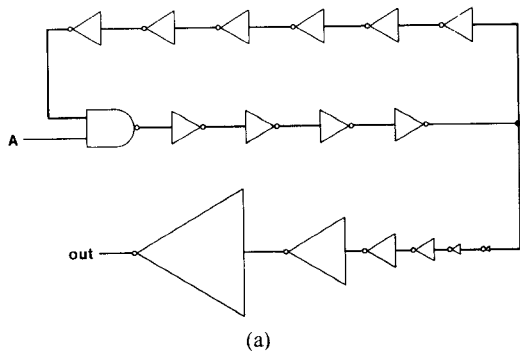


Fig. 1. (a) A block diagram of the ring oscillator is shown along with (b) the circuit diagram of one inverter.

critical parameters, or parameters which had the greatest effect on the output was selected. Based on these results a second group of simulations was performed using the variations in model parameters measured for the wafers from the two foundries. This was done to predict the range over which the measured frequency would be expected to vary. All simulations were performed using MOS2 in SPICE 2G.4 [7], [8], [12]–[14]. Simulated and measured waveforms are plotted in Fig. 2.

For the first group of simulations, all model parameters, including the channel lengths, the channel widths, the temperature, and the power supply voltages, were individually varied ± 10 percent about the measured mean and the frequencies recorded. This resulted in an ordered list of parameters ranked according to the sensitivity of SPICE to their variation. For this work, the critical parameters were defined as those which caused a frequency variation of more than 3.5 percent when the model parameter was varied. These critical parameters and the corresponding simulated frequency ranges obtained for the wafers from the two silicon foundries are listed in Table II. To obtain a realistic estimate of the effect that each critical parameter has on the frequency, for the processes used in this work, each parameter was also individually varied ± 1 measured standard deviation. The frequency results are also included in Table II.

To determine the range over which the measured frequency would be expected to vary, a second group of simulations was performed in which all of the critical

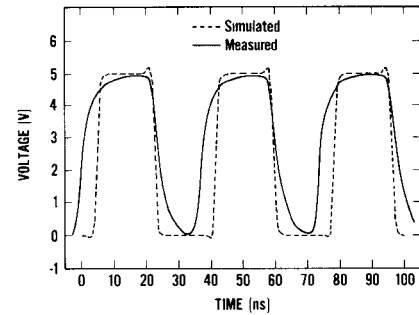


Fig. 2. The measured and simulated ring oscillator waveforms are plotted on the same axes.

TABLE II
A COMPARISON OF SIMULATED FREQUENCY RANGES (IN MEGAHERTZ) FOR SAMPLES FROM TWO SILICON FOUNDRIES WHEN THE INPUT PARAMETER IS VARIED ± 10 PERCENT OR $\pm \sigma$ (The parameters listed are the critical parameters because they cause a frequency variation of more than 3.5 percent when the parameter is varied ± 10 percent about its measured mean.)

Parameter	Foundry A		Foundry B	
	$\pm 10\%$ Range	$\pm \sigma$ Range	$\pm 10\%$ Range	$\pm \sigma$ Range
V_{DD}	7.9	—	8.2	—
L_p	6.7	2.4	8.6	2.6
L_n	5.2	2.9	6.9	3.5
t_{ox}	3.2	2.2	3.0	0.8
KP_n	3.2	0.4	3.6	0.7
LD	2.8	2.8	5.4	5.4
KP_p	2.6	0.4	3.4	1.4
W_n	2.0	0.2	2.1	.04
$VT0_n$	1.5	0.4	1.5	0.9
$CGD0$	1.3	1.8	1.9	2.6
$VT0_p$	1.1	0.2	0.7	1.1
Simulated Mean	29.7 MHz		35.6 MHz	

TABLE III
A COMPARISON OF MEASURED VERSUS SIMULATED MEAN VALUES AND RANGES FOR SAMPLES FROM TWO SILICON FOUNDRIES (Due to the low percent difference between the measured and simulated mean values, the intra-wafer mean of each parameter is a reasonable estimate of the actual model parameter. For the measured ring oscillator frequency range, the intra-wafer variations in the critical parameters provide an adequate model.)

	Foundry A	Foundry B
Measured Mean Value	30.7 MHz	34.3 MHz
Simulated Mean Value	29.7 MHz	35.6 MHz
Percent Difference in the Means	3.4 %	3.7 %
Measured Range	± 6.3 MHz	± 7.0 MHz
Simulated Range	± 7.0 MHz	± 9.9 MHz
Percent Difference in the Ranges	10.0 %	29.3 %

parameters were varied ± 1 standard deviation, representing the intra-wafer variations, and the highest and lowest frequencies determined. This approach assumes the parameters are statistically independent. These results are given and compared in Table III with actual measurements from ring oscillators on the wafer.

IV. DISCUSSION

Two types of deviations exist between the measured and simulated results. They are: 1) the differences between the measured frequency mean and the simulated frequency

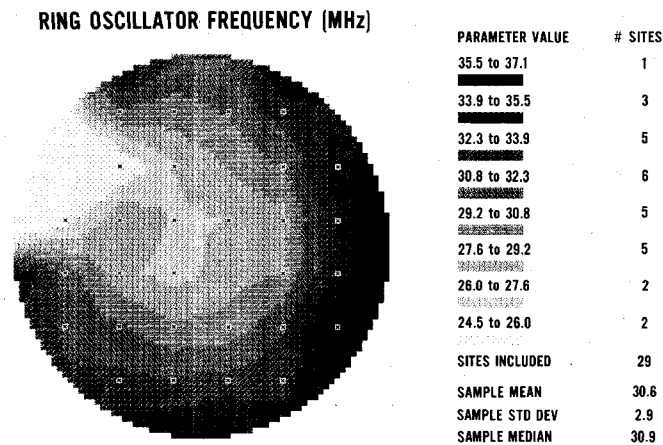


Fig. 3. A ring oscillator frequency wafer map shows the test site locations and the intrawafer parameter variations. An approximate inverse correlation exists between the ring oscillator frequency and the polysilicon gate linewidth, Fig. 4, suggesting that the channel length variation is the primary cause of the frequency variation.

utilizing the mean values of all the model parameters, and 2) the simulated range in which the measured results are expected to be found and the actual measured range.

Several factors can cause differences between the simulated and measured results. The first type of deviations can be due to the inaccuracy of the SPICE model, deficiencies in the design of test structures used for extracting the SPICE parameters, and deficiencies in measurement methods. The results given in Table III for the two silicon foundries show close agreement between the measured and simulated means.

The second type of deviations can be due to intrachip and intrawafer parameter variations which result from processing variations over the wafer. In Table III, the measured range of values is compared to the simulated range. For this work, the simulated range is obtained by using the critical model parameters with their corresponding measured standard deviation, or intrawafer variations, which produce the highest and lowest frequencies. Hence, the assumption that the parameters are statistically independent yields a worst case range. Therefore, the simulated range is larger than the measured range.

A wafer map illustrating the intrawafer ring oscillator frequency variations for the sample from foundry A is shown in Fig. 3. The map was produced using STAT2 [6]. To identify the cause of these frequency variations, wafer maps were made for several critical input parameters. A polysilicon gate linewidth wafer map is shown in Fig. 4 for structures designed to have a linewidth of 8.0 μm . It is assumed that the same variation would exist for 5- μm structures. An approximate inverse correlation exists between the polysilicon gate linewidth, also called the channel length, and the ring oscillator frequency suggesting that the channel length variation is the primary cause of the frequency variation. To support this conclusion, transconductance wafer maps for n- and p-channel MOSFET's, shown in Figs. 5 and 6, respectively, show an approximate inverse correlation with the channel length. It is, therefore, concluded that the principle cause of the intrawafer frequency variation is the intrawafer polysilicon gate

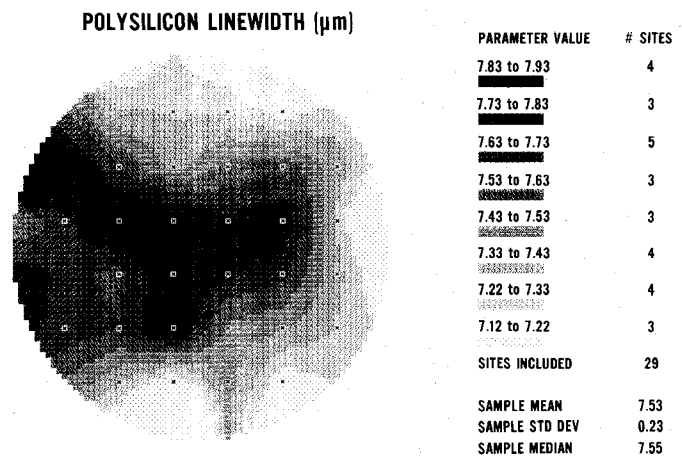


Fig. 4. A polysilicon gate linewidth wafer map shows the test site locations and the intrawafer parameter variations.

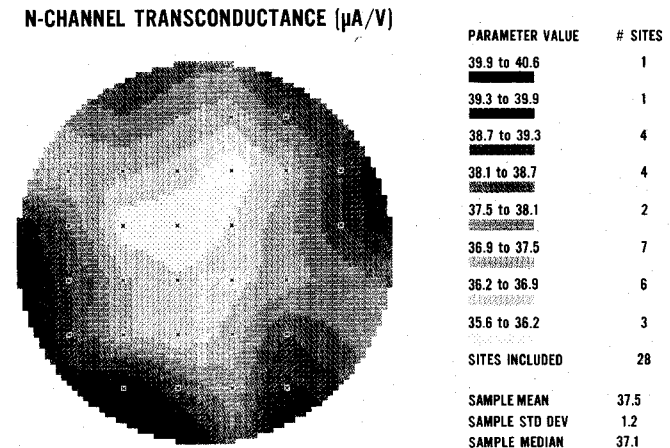


Fig. 5. A transconductance wafer map for an n-channel MOSFET shows the test site locations and the intrawafer parameter variations. An approximate inverse correlation exists between the transconductances (n- and p-channel) and the channel length supporting the conclusion that the principle cause of the intrawafer frequency variation is the intrawafer polysilicon gate linewidth variation which in turn causes a corresponding variation in the n- and p-channel transconductances.

linewidth variation which in turn causes a corresponding variation in the n- and p-channel transconductances. To obtain tighter control on the circuits performance and hence increase the reliability of the process, it is important to minimize polysilicon linewidth variations across a wafer.

Variations of a given parameter within a chip (intrachip variations) can lead to differences between the model parameters measured and their corresponding value in the actual circuit. To estimate the magnitude of these differences, identical MOSFET's placed across a test chip were tested and the intrachip variations in selected critical parameters measured. The devices probed in these MOSFET arrays had a channel length of 8.0 μm and a channel width of 77.0 μm . Ten n-channel and ten p-channel arrays were placed across each test chip. The wafer was arranged such that six test chips were evenly spaced across the diameter of the wafer. Data values from the 8.0- μm devices are taken from all of the MOSFET's across the diameter of the wafer. The n- and p-channel transconductances are plotted as a function of wafer position in Figs. 7

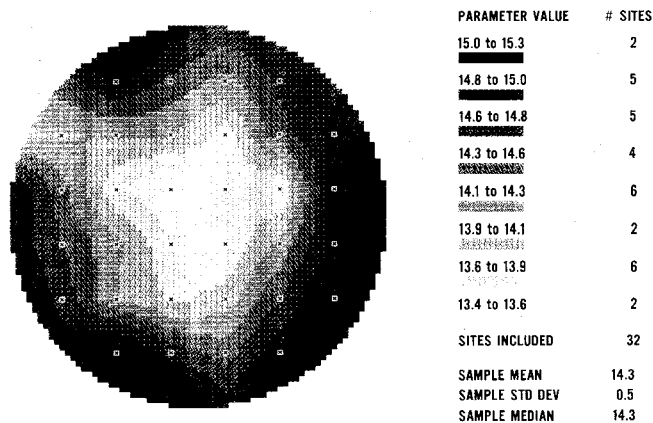
P-CHANNEL TRANSCONDUCTANCE ($\mu\text{A}/\text{V}$)

Fig. 6. A transconductance wafer map for a p-channel MOSFET shows the test site locations and the intra-wafer parameter variations.

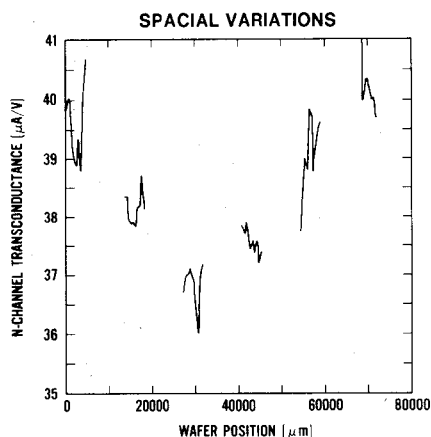


Fig. 7. The n-channel transconductance is plotted against the position across the diameter of a wafer. While the overall intra-wafer variation is similar to that seen in Fig. 5, an intrachip variation in the parameter is also observed. The measured intrachip variations suggest that SPICE simulations can be influenced by the intrachip variation in the critical input parameters.

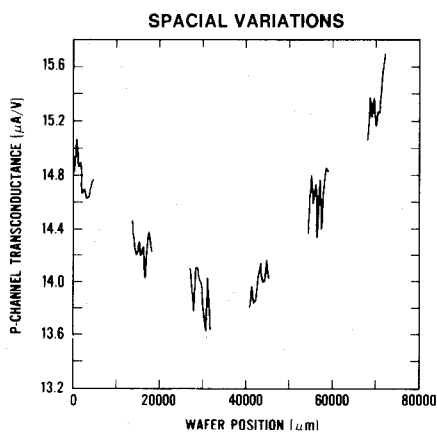


Fig. 8. The p-channel transconductance is plotted against the position across the diameter of a wafer.

and 8, respectively. While the overall intra-wafer variations seen in Figs. 7 and 8 are similar to those seen in their corresponding wafer maps, Figs. 5 and 6, an intrachip variation in the parameter is also observed. To identify the cause of these variations, further analysis involving addi-

tional test structures is needed. The measured intrachip variations suggest that SPICE simulations can be influenced by the intrachip variation in the critical input parameters.

V. CONCLUSIONS

A sensitivity analysis was performed and the critical parameters, which are shown in Table I, were identified and then measured. The intra-wafer variations of these parameters are sufficient for determining the range within which to expect the measured frequency of a ring oscillator. The magnitude of the simulated range is approximately the magnitude of the spread of the frequency data. Intra-wafer process variations account for this range in the measured frequency results.

Due to the lack of proximity between the test structures from which the SPICE parameters are obtained and the ring oscillators, intrachip variations can cause a difference between the measured and simulated ring oscillator frequency.

The conclusions that can be drawn from this work based on the samples tested are: 1) there is a subset of the total SPICE parameters which have the greatest effect on the simulation; 2) the intra-wafer mean of each parameter is a reasonable estimate of the actual model parameter; and 3) the intra-wafer variations in the critical parameters can account for a frequency range that is approximately equal to the measured frequency range. For the samples tested, it was determined that: 1) the polysilicon gate linewidth is indirectly proportional to the frequency and was the primary cause of the frequency variation; and 2) intrachip parameter variations can influence SPICE sensitivity.

ACKNOWLEDGMENT

The author would like to especially acknowledge the contributions of L. W. Linholm to this project. For comments on this paper, she would like to thank D. L. Blackburn, K. F. Galloway, T. F. Leedy, H. E. Marshall, H. A. Schafft, E. J. Walters, and C. L. Wilson from the National Bureau of Standards and H. C. Lin from the University of Maryland. She would also like to thank M. Gaitan and J. S. Suehle, also from the National Bureau of Standards, for obtaining the device model parameters for SPICE. The help of all others involved with this work is appreciated. Fabrication services from the MOSIS system, University of Southern California/Information Sciences Institute and from the Jet Propulsion Laboratory are also appreciated.

REFERENCES

- [1] T. W. Griswold, "Portable design rules for bulk CMOS," in *VLSI Design III*, no. 5, 1982, pp. 62-67.
- [2] M. G. Buehler, S. D. Grant, and W. R. Thurber, "Bridge and van der Pauw sheet resistors for characterizing the linewidth of conducting layers," *J. Electrochem. Soc.*, vol. 125, pp. 650-654, 1978.
- [3] M. G. Buehler and L. W. Linholm, "Role of test chips in coordinating logic and circuit design and layout aids for VLSI," *Solid State Technol.*, vol. 24, no. 9, pp. 68-74, Sept. 1981.

- [4] M. G. Buehler, "Comprehensive test patterns with modular test structures: The 2 by N probe pad array approach," *Solid State Technol.*, vol. 22, no. 10, pp. 89-94, Oct. 1979.
- [5] R. L. Mattis and M. R. Doggett, "A microelectronic test pattern for analyzing automated wafer probing and probe card problems," *Solid State Technol.*, vol. 21, no. 11, pp. 76-79, Nov. 1978.
- [6] R. L. Mattis, *Semiconductor Measurement Technology: A FORTRAN Program for Analysis of Data from Microelectronic Test Structures*, NBS Special Pub. 400-75, July 1983.
- [7] A. Vladimirescu and S. Liu, "The simulation of MOS integrated circuits using SPICE2," Electronics Research Lab., Univ. of California, Berkeley, CA, Memo. ERL-M80/7, Feb. 1980.
- [8] D. R. Alexander, R. J. Antinone, and G. W. Brown, *SPICE2 MOS Modeling Handbook*, BDM/A-77-071-TR, The BDM Corp., Albuquerque, NM, May 1977.
- [9] K. Terada and H. Muta, "A new method to determine effective MOSFET channel length," *Japan J. Appl. Phys.*, vol. 18, pp. 953-959, May 1979.
- [10] N. Sasaki, "Higher harmonic generation in CMOS/SOS ring oscillators," *IEEE Trans. Electron Devices*, vol. ED-29, pp. 280-283, Feb. 1982.
- [11] H. C. Lin and L. W. Linholm, "An optimized output stage for MOS integrated circuits," *IEEE J. Solid-State Circuits*, vol. SC-10, pp. 106-109, Apr. 1975.
- [12] L. W. Nagel, "SPICE 2: A computer program to simulate semiconductor circuits," Electronics Res. Lab., Univ. of California, Berkeley, CA, Memo. ERL-M510, May 1975.
- [13] E. Cohen, "Program reference for SPICE2," Electronics Res. Lab., Univ. of California, Berkeley, CA, Memo. ERL-M592, June 1976.
- [14] W. J. McCalla and D. O. Pederson, "Elements of computer-aided circuit analysis," *IEEE Trans. Circuit Theory*, vol. CT-18, pp. 14-26, Jan. 1971.



Janet M. Cassard received the B.S. degree (magna cum laude) in physics from Muhlenburg College, Allentown, PA, in 1978 and the M.S. degree in electrical engineering from Lehigh University, Bethlehem, PA, in 1981.

In 1978, she joined Bell Laboratories in Allentown where she initially investigated the oxidation kinetics of NiZn ferrites. In 1979 she joined the 64K dynamic RAM design team and later the 256K dynamic RAM design team giving special attention to the back-gate bias generator. She is currently involved with the design of dynamic integrated-circuit test structures for the Semiconductor Devices and Circuits Division at the National Bureau of Standards, Washington, DC.

(End of Special Papers Section.)

Regular Papers

Techniques for a 5-V-Only 64K EPROM Based Upon Substrate Hot-Electron Injection

JAMES L. McCREARY, MEMBER, IEEE, BOAZ EITAN, MEMBER, IEEE, AND DANIEL AMRANY

Abstract—A 64K EPROM based upon substrate hot-electron injection was designed and fabricated. 5-V-only programming was demonstrated by on-chip charge pumps. The typical programming rate was approximately 1 V/ms. Sense amplifier improvements provided 4-mV offset, 52-dB PSRR, and 60-dB CMRR.

I. INTRODUCTION

CONVENTIONAL EPROM products have demonstrated the manufacturability and reliability of the channel-hot-electron programming technique. Program-

ming cycle time less than 20 ms and better than 10-year retention are now industry standards. This paper describes the evaluation of a 5-V-only 64K EPROM based upon substrate hot-electron programming.

Conventional EPROM's use the method of channel hot-electron (CHE) programming. This involves the generation of hot-electrons in the high-field region between the pinched-off channel and the drain. Electrons with sufficient energy have a small probability of being injected across the thin oxide to the floating gate, thereby programming the device (increasing the threshold voltage). The efficiency of this injection process is low. This may be improved by applying large drain and gate voltages, but this results in high drain current. Consequently, one disadvantage of the CHE approach is that it does not allow 5-V-only operation but requires external high-voltage sup-

Manuscript received July 28, 1983; revised September 29, 1983.

J. L. McCreary was with the Intel Corporation, Santa Clara, CA 95051. He is now with the Micro-Linear Corporation, Sunnyvale, CA 94087.

B. Eitan was with the Intel Corporation, Santa Clara, CA 95051. He is now with Wafer Scale Integration, Santa Clara, CA 95050.

D. Amrany is with the Intel Corporation, Santa Clara, CA 95051.